Research article

Maik Pflugradt*, Steffen Mann, Viktor Feller, Yirong Lu and Reinhold Orglmeister

Online learning algorithms for principal component analysis applied on single-lead ECGs

Abstract: This article evaluates several adaptive approaches to solve the principal component analysis (PCA) problem applied on single-lead ECGs. Recent studies have shown that the principal components can indicate morphologically or environmentally induced changes in the ECG signal and can be used to extract other vital information such as respiratory activity. Special interest is focused on the convergence behavior of the selected gradient algorithms, which is a major criterion for the usability of the gained results. As the right choice of learning rates is very data dependant and subject to movement artifacts, a new measurement system was designed, which uses acceleration data to improve the performance of the online algorithms. As the results of PCA seem very promising, we propose to apply a single-channel independent component analysis (SCICA) as a second step, which is investigated in this paper as well.

Keywords: blind source separation; body sensor network; ECG processing; home monitoring; movement artifacts; Neural Netwoks; online PCA; single-channel ICA (SCICA).

*Corresponding author: Maik Pflugradt, Chair of Electronics and Medical Signal Processing, TU Berlin, Berlin, Germany, E-mail: Maik.Pflugradt@tu-berlin.de
Steffen Mann, Viktor Feller, Yirong Lu and Reinhold Orglmeister: Electronics and Medical Signal Processing, TU Berlin, Berlin, Germany

Introduction

Principal component analysis (PCA) is a widely accepted method in statistical data analysis with respect to dimension reduction, feature extraction, data decorrelation, and whitening [14]. Moreover, PCA is usually performed as a preprocessing step to independent component analysis (ICA), which, itself, is commonly used in the applications of blind source separation (BSS). In biosignal processing, statistical calculations like PCA and ICA, have gained increasing popularity in the past decades [6]. It has also been shown that even from a single-lead ECG, valuable information like morphologic variability, ventricular repolarization, atrial fibrillation or myocardial ischemia can be extracted by PCA [3]. Langley et al. have used PCA by eigenvalue and eigenvector decomposition to extract an ECG-derived respiration feature from a single-lead ECG [2, 16].

The PCA problem can be stated as follows. Find an orthogonal transformation matrix $\mathbf{A}$ such that the elements of the centered measurement vector $\mathbf{x}$ become uncorrelated:

$$\mathbf{y} = \mathbf{A}\mathbf{x}. \tag{1}$$

Thus, the covariance matrix of the transformed data set $\mathbf{y}$ is diagonal. It can be shown that PCA is equivalent to the variance maximization of the principal components (PCs), which are represented by the elements of $\mathbf{y}$ and that the solution of maximizing the variance is given by the unit-length eigenvectors of the covariance matrix $\boldsymbol{C}_x$ of $\mathbf{x}$ [14]. Because of nonstationarity, it would be necessary to reestimate $\boldsymbol{C}_x$ and recalculate the eigenvectors periodically, which can be critical when high-speed processing of on line-arriving data samples is needed. This makes adaptive, computationally efficient online learning algorithms very attractive. Gradient algorithms based on the neural networks' (NN) learning rules allow the estimation of the eigenvectors without using second-order statistics at all [13]. It is also known that the more sophisticated ICA calculations can be implemented with the help of efficient online approaches [13], which has also attracted the attention of this paper.

In [18], we have evaluated different learning algorithms in an attempt to extract respiratory activity out of single-lead ECGs acquired from the Physionet Database. As the results were quite promising, we decided to develop a new measurement system consisting of a wireless multichannel ECG sensor-module in combination with a piezo respiration belt sensor-module. This enables us to collect specific data sets and to gain quantitative results that help to evaluate the performance of the discussed approaches. In our study, we carried out dedicated experiments to investigate the influence of movement artifacts on the learning processes of the estimated eigenvectors. It turns out that the additional acquired three-axis acceleration signals acquired by our hardware can be used to

significantly improve the outcome of the suggested algorithms. Moreover, we devised special measurement procedures that aimed at detecting interruptions in breathing – which might be helpful when dealing with apnea – and in tracking different breathing rates out of the single-lead ECGs. Especially, therapies in the field of sleep medicine could greatly benefit from the online calculated results, as it might be possible to abstain from additional respiratory hardware completely.

The paper is organized as follows. In the first part of Theoretical backgrounds, we briefly depict the underlying PCA neural network layer, which is used to implement the individual learning algorithms. It is also shown that this software framework can be flexibly used for adaptive ICA implementations.

In the second part of that section, a short overview of the selected gradient ascent algorithms and their respective learning rules is given, whereas the third part concerns itself with the specific ECG processing approaches. Methodology introduces the data sets from the Physionet database and depicts the elaborated experimental setups, which were used to collect unique laboratory records. This part is followed by a short presentation of the beforementioned innovative measuring system emphasizing its capabilities and special features. The obtained results are presented and discussed in the second part of that paper, where the performance of the different algorithms is studied and possible applications of PCA and ICA applied to single-lead ECG data are evaluated. The last section finishes with the summarized conclusions.

Theoretical backgrounds

PCA neural network

A neat way for the online computation of the PCA expansion has been proposed by Oja, who introduced an artificial NN as an adaptive system layer that receives online-arriving streaming data and estimates the PCs [17]. This idea has led us to build a linear PCA layer as shown in Figure 1, which is used to implement the algorithms described in the next subsection. A global PCA object can contain several NN objects, which are, themselves, configurable by numerous neuron objects. Therefore, it is easily possible to implement arbitrary network configurations like multilayer and feedback structures. As there are also adaptive solutions to the ICA problem, which are based on the gradient algorithms estimating and minimizing measures of non-Gaussianity like kurtosis or negentropy [13], the proposed framework can be used for these tasks as well.

Learning algorithms

The learning algorithms work as an iteration process on the data set where the weight vectors, w_i, are adjusted in each step and finally converge to the corresponding eigenvectors. The gradient algorithm finds the local minima in a multidimensional contrast function, $\psi(w)$, with the help of the update rule

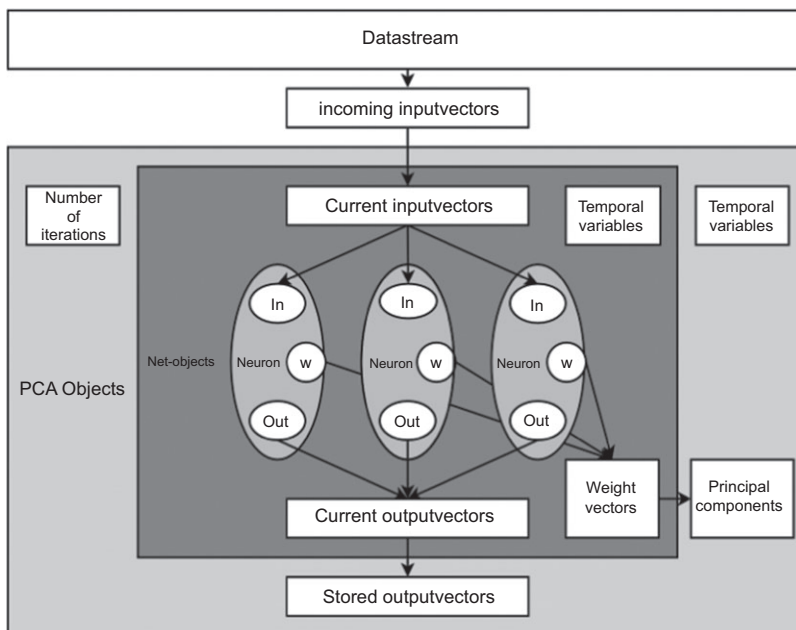**Figure 1** The PCA NN layer used by the online learning algorithms.

$$w(t) = w(t-1) - \frac{\alpha(t)(\partial \psi(w))}{\partial w}, \qquad (2)$$

in which $\alpha(t)$ specifies the learning rate. In the scope of this study, we selected five well-established learning rules from literature for implementation.

The stochastic gradient ascent (SGA) approach, which was introduced by Oja [17], can be seen as the pioneering work to implement an online computation of the PCA expansion. Basically, the gradient of the variance y_1^2 is estimated with respect to the weight vector w_1, which results in the general learning rule expressed in Equation 3 [17].

$$\Delta w_j = \gamma y_j \left[x - y_j w_j - 2 \sum_{i<j} y_i w_i \right]. \qquad (3)$$

A modification of this learning rule resulted in the generalized Hebbian algorithm (GHA) by Sanger [23], who revised the deflationary approach to calculate the minor components. An attempt to calculate all the components in parallel by using lateral connections within the NN was proposed by Kung et al. in their APEX algorithm [15]. Using a recursive least squares (RLS) principle to enhance the convergence behavior, which depends on the learning rate, has been suggested in the PASTd algorithm introduced by Yang [25]. In this work, we have also evaluated a relatively new learning algorithm, which promises fast convergence speed and robust stability [22].

In [9], the authors provide a real-time PCA (RTpca) implementation based on a DSP system to implement the following learning algorithm,

$$w(n+1) = (1-T) w(n) + T \frac{num(n)}{den(n)}, \qquad (4)$$

$$y(n) = w^T(n) x(n), \qquad (5)$$

with

$$num(n) = \left(1 - \frac{1}{n} \right) num(n-1) + \frac{1}{n} x(n) y(n), \qquad (6)$$

$$den(n) = \left(1 - \frac{1}{n} \right) den(n-1) + \frac{1}{n} y^2(n). \qquad (7)$$

Here, $T \in [0; 1]$ is the parameter that determines the convergence speed.

All considered algorithms have linear complexity. The point of interest focuses on the estimated eigenvectors, which are compared against those gained by the classical closed-form computation of the covariance matrix, C_x. At this stage, all the algorithms have been implemented in MATLAB. No sophisticated functions have been used so that porting them to C should be an easy task.

Online ECG processing

In the first step of the processing chain, a multidimensional observation matrix is extracted from each sampled ECG channel. This is done by extracting a segment of N samples adjusted by the corresponding QRS complex. This step is iterated over a set of M QRS complexes, resulting in an $N \times M$ observation matrix **X**, which can be seen as the realizations of the random process **x**.

The window length N has a significant influence on the behavior of the algorithms [3]. With respect to the ECG-derived respiration, Langley et al. pointed out that a segment size containing the length of a QRS complex provided the best results [16]. In the scope of this study, we also found extracting a whole QRS complex to be most promising and, therefore, set the window size to $N=41$ samples (164 ms).

When working with the data sets downloaded from the Physionet Database, the professionally annotated QRS complexes have been used. When processing our own data sets, we have been using a filterbank algorithm for reliable QRS complex detection [1].

Castells et al., then, propose to calculate the $M \times M$ correlation matrix

$$\hat{R}_x = \frac{1}{M} XX^T, \qquad (8)$$

whose PCs can be used to extract an intrabeat correlation. They also suggest to calculate an $N \times N$ correlation matrix

$$\bar{R}_x = \frac{1}{N} X^T X, \qquad (9)$$

which, after PCA decomposition, yields an interbeat correlation of the ECG signal [3]. Both approaches require the full data set to be available when calculating the correlation matrices. This makes an online calculation impossible and requires a computationally complex recalculation of the correlation matrices and its subsequent PCA expansion every time a new sample is added.

In our approach, we overcome this problem by feeding the earlier-mentioned learning algorithms one QRS block at a time, yielding an adaptive estimation of the eigenvectors. If this approach turns out to work flawlessly, one could estimate the PCs of $\hat{R}_x$ online and, thereby, track the morphological changes in the ECG beat signals. An online estimation of the PCs derived from $\bar{R}_x$

is not possible though, as the whole data set would be needed again.

In order to evaluate the estimation process of the learning algorithms, we introduce the following two criteria.

Approximation error

$$e_{appr} = \left\| \boldsymbol{\nu}_i - \frac{\boldsymbol{w}_i}{\|\boldsymbol{w}_i\|} \right\|. \tag{10}$$

Orthonormality error

$$e_{orth} = \sum_{i=1}^{n} \sum_{j=1}^{n} \left(\boldsymbol{w}_i^T \boldsymbol{w}_j \right)^2, \quad i \neq j. \tag{11}$$

The approximation error, e_{appr}, sums up the absolute difference of the angle spanned by the ith eigenvector, $\boldsymbol{\nu}_i$, calculated by the traditional eigenvector decomposition of the covariance matrix and the corresponding ith eigenvector, $\boldsymbol{w}_i$, estimated by the learning algorithm. It is principally accepted that the proposed PCA learning algorithms have problems in estimating the minor PCs [13]. As a large part of the ECG signal energy is concentrated on the first PCs, we only concentrate on estimating the first four eigenvectors. As it is also the case that the order of the eigenvectors is mixed up during the adaption process, the approximation error, e_{appr}, is prone to wrong pairing of $\boldsymbol{w}_i$ and $\boldsymbol{\nu}_i$. Therefore, we defined an additional criterion, the orthonormality error, e_{orth}, which is calculated by the dot product of the estimated eigenvectors. In addition to these values for the proper assessment of the algorithms, one has to consider the number of iteration steps needed until convergence is reached.

Further, it can be shown that some learning algorithms are able to estimate the eigenvalue [5]. With respect to the RTpca algorithm, one can easily show that $num(n)$ in Equation 6 will converge to

$$\frac{1}{n} \sum_{k=1}^{n} y_1^2(k), \tag{12}$$

which corresponds to the variance of the projected elements.

The main notion of this paper is to suggest a suitable learning algorithm to analyze multiple single-channel ECGs. Using this approach, we can provide online calculations – being the central innovation of this paper – of the initially mentioned single-channel PCA applications like adaptive respiratory activity extraction.

Processing contigious blocks, extracted from single-channel signals as discussed so far, has also been proposed in the single-channel ICA (SCICA) application presented in [7]. Assuming disjoint spectral support of the stationary sources, one can extract independent components out of the observation matrix. Hyvärinen has introduced a computationally efficient fixed-point algorithm, called fastICA, which extracts the ICs by maximizing the kurtosis or negentropy of the observation signals [11, 12]. Hyvärinen also shows that the kurtosis and negentropy can be estimated by the gradient algorithms allowing adaptive implementations for the problem as well. Thus, we also apply the SCICA approach in the scope of this work.

Methodology

Data sets

For a better reproducibility of the conducted signal processing tasks, data sets of single-lead channels were obtained from the Fantasia Database of Physiobank ATM, which provides a single-channel ECG and a respiratory signal sampled at 250 Hz [19]. As no special experiments were carried out in these data sets, records of 10-min duration were arbitrarily chosen. Unfortunately, such data is not always suited for specific research, as the environmental circumstances and other important details are sometimes unknown or incomplete.

To further investigate the drawbacks and opportunities of the discussed applications, we initialized a small field study of 50 healthy subjects. Each proband took part in three different experiments, which are presented in more detail in the next subsection.

Principally, these experiments aimed at three points. First, we wanted to evaluate and compare the performance of the proposed algorithms in terms of accuracy and convergence speed. For that reason, data sets from Physionet have been referred to. Second, it is well known that signal disturbances induced by movement artifacts generally impede biosignal processing tasks and also severely hamper the estimation processes as will be shown in this paper. For that reason, we included coordinated measurements with typical movement artifacts. As the acceleration data is also recorded with our sensors, we have a valuable reference that can help to significantly improve the performance of the adaptive algorithms. Finally, we have special interest in the online tracking of respirational activity. On this account, the measurements included different breathing patterns and predetermined breath interruptions.

Measurement system

In preparation of the conducted laboratory experiments, we developed a new wireless sensor system that allows us to sample a three-channel ECG and a respiratory signal simultaneously [10, 21].

The sensor nodes consist of a very energy-efficient MSP430F1611 (Texas Instruments, Dallas, TX, USA) microcontroller [24], a CC2500 (Texas Instruments, Dallas, TX, USA) low-power 2.4-GHz RF transceiver, a three-axis ADXL330 (Analog Devices, Norwood, MA, USA) accelerometer, and an SD card for data storage. The ECG sensor is equipped with an *ADS1298* (Texas Instruments, Dallas, TX, USA) analog ECG/EEG front end that allows multiple-channel ECG sampling, which is based on 24-bit delta-sigma analog-to-digital converters with built-in programmable gain amplifiers. Respiration is obtained by a sensor module using a medical piezo respiration belt from VERMED. ECG, respiration, and the acceleration data are sampled at 250 Hz. The energy consumption of one sensor in active measurement mode was determined around 100 mW, which guarantees operation of almost 48 h when driven by a small-size lithium ion battery, typically used in mobile phones. The measurement setup is shown in Figure 2.

Experimental setup

In the scope of this study, 50 healthy subjects (70% male, 30% female, ages 21–52 years) have volunteered to take part in a three-measurement experiment to acquire a three-lead ECG according to Einthoven as well as a respiratory signal recorded by a respiratory piezo belt, which is worn on the lower left side of the thorax.
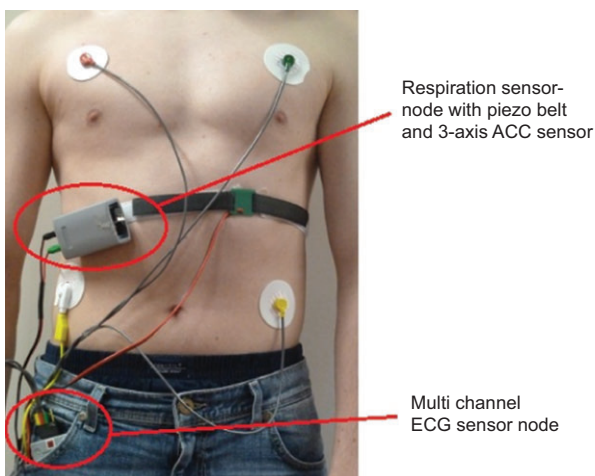

Respiration sensor-node with piezo belt and 3-axis ACC sensor

Multi channel ECG sensor node

Figure 2 The measurement system consisting of a three-channel ECG sensor and a respiratory belt sensor.

Experiment I

In the first measurement, all the subjects were asked to follow four different breathing patterns in a sitting position. This measurement was conducted over a duration of 10 min. In the first 2 min, the subjects were asked to breathe normally, followed by the four 2-min intervals were a specific breathing frequency of either 10, 12, 15, or 20 breaths per minute (bpm) should be followed that has been supplied in the form of a real-time sinewave plot inside a MATLAB script. The order of the different breathing frequencies was randomly changed for each measurement.

Experiment II

Next, a measurement in the supine position extending over a period of 7:45 min has been conducted. After exactly 4 min, the subjects were asked to stop breathing for 15 s, followed by two consecutive 60 s of normal breathing and 15 s of holding breath periods, concluded by a last minute of normal breathing.

Experiment III

The last recording is comprised of an 8-min period while quietly sitting at the desk, with two interruptions of standing up, walking for 5 s to induce the movement artifacts and sitting down again. Figure 3 plots a fragment of each measurement, showing the respiratory signal and ECG lead II together with the offline-detected QRS complexes. In the third plot, the acceleration data is provided as well, which is a valuable reference to adjust the configurations of the learning algorithms, as will be shown in the results section.

One serious drawback of the single-channel approach is the dependence on the QRS complex detection performance, which, in turn, crucially depends on the signal quality. The third plot in Figure 3 already provides a slight impression of the influences of the movement artifacts. Therefore, we carefully investigate the adaption behavior of the selected algorithms within such critical time episodes. Here, experiment III is of special interest, as these data sets show motion artifacts at known time periods supplied with a three-channel acceleration signal that serves as a further reference. This knowledge is then used to derive solutions that significantly strengthen the robustness and performance of the learning algorithms. It should be noted that the respiration reference signal is
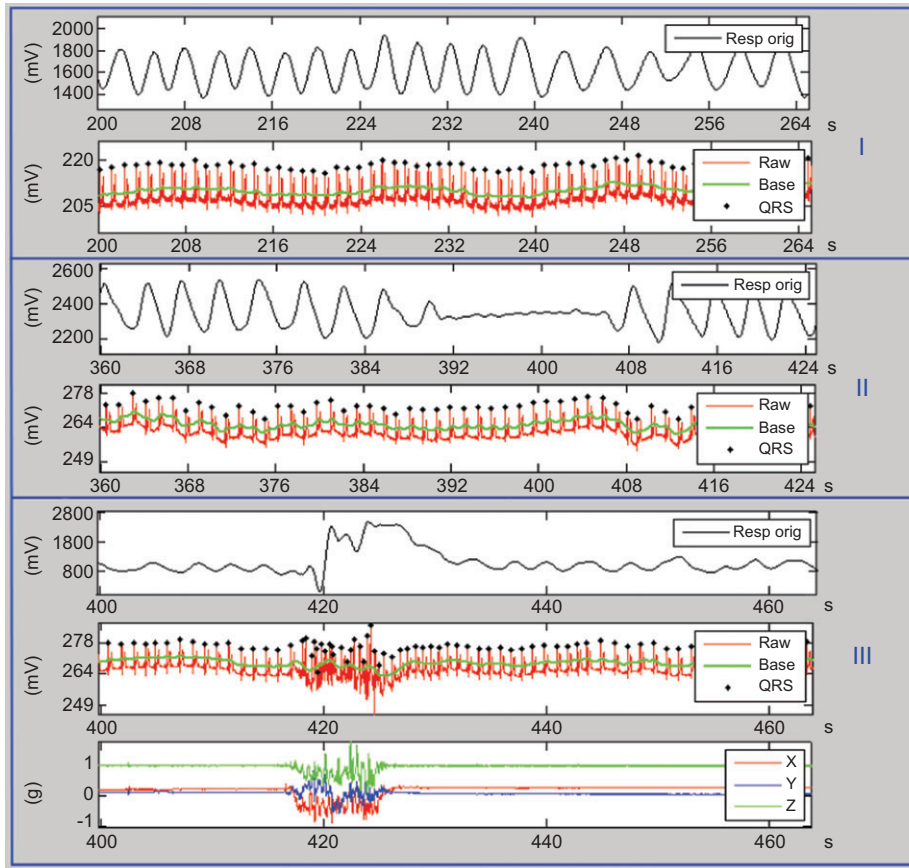
Figure 3 The raw signals (sampling frequency: 250 Hz) – Experiment I: subjects had to follow different breathing rates. Experiment II: subjects were asked to stop breathing at intervals. Experiment III: movement artifacts and ACC signals.

also strongly affected by motion artifacts, as a piezo belt is not a very robust construction. In experiments I and II, no artifacts are occurring, providing a nondisturbed reference signal in our database. These records are used to test the algorithms on their ability to determine changing breathing frequencies and stops in breathing.

Results

The results of the initial performance tests evaluating the different algorithms are summarized in Table 1. The overall performance of a specific algorithm depends on multiple factors, namely, the initialization of the weight vectors, the implementation of the learning rate and its initial value, the block length of the extracted segments, and the signal quality. In this test, 100 measurements on the five data sets of the Physionet Fantasia record have been used. Each data set was processed 20 times by each algorithm with random starting points of the weight vectors and changing block sizes (including either the QRS complex or the whole beat). A threshold of 0.1 of the approximation error, e_{appr} (Equation 10), was set as a global criterion that determined convergence. The average number of the iteration steps needed by the corresponding algorithm to achieve convergence on a specific data set is recorded in Table 1. As can be clearly seen, the RTpca algorithm seems to outperform the other algorithms with respect to the number of estimated PCs and convergence speed. We deliberately chose arbitrary data sets out of the Physionetbank, which contained a certain degree of artifacts and were not preprocessed. Applying the algorithms on data sets without artifacts will considerably improve the results of all the algorithms, although RTpca still performs best. It should be mentioned again that the performance could significantly change when adjusting the learning rates. At this point, we cannot preclude that there might be a configuration that outperforms the above-presented results. Nonetheless, the RTpca results are very satisfying and convinced us to select the RTpca algorithm for the following analysis.

Table 1 Performance of the different algorithms applied on the five data sets from Physionet Fantasiabase. All the values are averaged over 20 calculations on the same data set with slightly changing configurations (block size, initialization). Each cell contains the number of iterations that have passed to estimate the corresponding principal component PC1/PC2/PC3/PC4. No value means that the corresponding PC could not be estimated.

Record	SGA	GHA	APEX	PASTd	RTPCA
f1o10	45/95/-/-	99/173/-/-	**30**/152/-/-	121/240/650/-	**61/158/288/685**
f1y01	88/97/-/-	101/158/-/-	131/187/-/-	127/302/551/-	**34/121/332/721**
f1y09	23/55/-/-	54/103/-/-	58/95/-/-	77/201/499/-	**15/61/82/890**
f2o03	55/87/-/-	74/130/-/-	99/205/-/-	84/225/600/-	**47/99/220/643**
f2o09	77/132/-/-	95/147/-/-	113/215/-/-	97/198/540/-	**65/131/198/732**

Bold indicates the best results.

As indicated, the movement artifacts have a significant influence on the signal quality and, therefore, might also disturb the learning process considerably. In order to draw a statistically significant conclusion, we analyzed the convergence behavior of the eigenvectors estimated from the data sets of Experiment III as discussed in previous section. Moreover, we made sure to keep the learning rate at a small constant value to retain the ability to track nonstationary statistics. In Figure 4, we plotted the lengths of the first four estimated eigenvectors along with the sampled ACC signals. Usually, the eigenvectors tend to have unity in length when converging against the plausible results. Apparently, the environmental change of the system leads to a reorientation of the estimation process, as can be seen by the spikes, which coincide with the activity in the ACC signal.

A Student's t-test was run over all the 50 data sets, which confirmed a statistical significance in the changing energy of the ACC signal when spikes in the eigenvector estimation have been detected. As a p-value of 3.27×10^{-14} has been obtained, the null hypothesis (no correlation between the ACC spikes and the EV spikes) can be discarded.

A major focus has been the extraction of respiratory activity out of the single-lead ECG. Therefore, Experiment

I was designed to determine the ability of the learning algorithm RTpca to detect the respiratory signal as was described in subsection Experimental Setup. Experiment I consists of five periods with different breathing rates. The first period was ignored, which contains the arbitrary respiration patterns. Thus, each record provides four separate samples of 2 min each. As the time intervals are known, the corresponding 2-min intervals have been extracted from ECG I, ECG II, and the reference respiratory signal, respectively. Next, the PCs have been calculated offline using the singular value decomposition (SVD) [8], and the online RTpca algorithm was applied to estimate the PC containing the respiratory activity. In [16], it was already shown that the offline SVD achieves good results in respiratory signal extraction. To double check, we compared the estimated PC by RTpca with the calculated PC by SVD, on the one hand and the estimated PC with the reference signal on the other hand. Therefore, the magnitude squared coherence, Coh_{xy}, and the correlation as the maximum of the crosscorrelation of the estimated PC and the reference breathing signal have been determined.

$$Coh_{xy} = \max\left(\frac{|P_{xy}(f)|^2}{P_{xx}(f)P_{yy}(f)}\right). \tag{13}$$

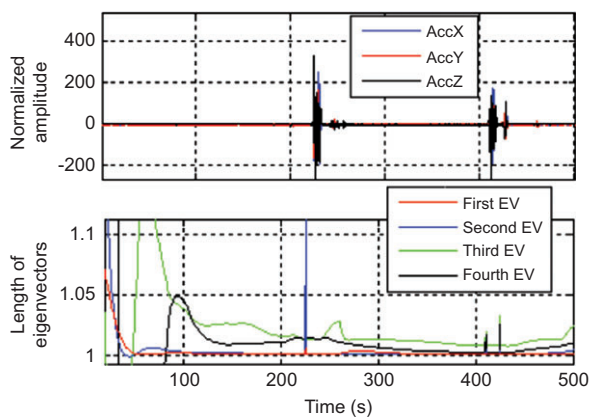$$Cor_{xy} = \max\left(\sum_{n=0}^{N \cdot m-1} x_{n+m} y_n\right). \tag{14}$$

The extracted time signal is shown in Figure 5, using a spline interpolation to plot the graph, whereas Figure 6 summarizes the obtained results by the different algorithms, based on the 50 data sets (which will sum up to 200 2-min samples) of our study. As can be extracted from the values summarized in the boxplot, the performance of the RTpca learning algorithm yields satisfying results in terms of respiratory signal extraction.

As another sample application of how the dynamics of the online-calculated eigenvectors can be used to track the changes in the breathing, the alterations in the
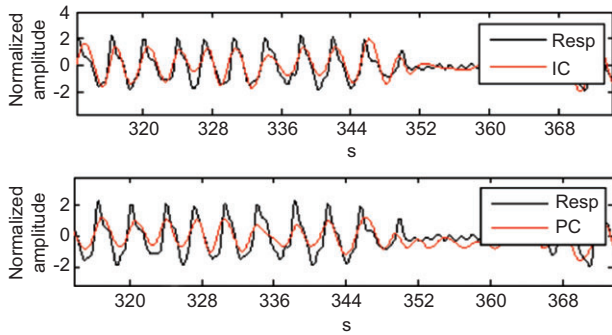

Figure 4 The eigenvector corruption during the ACC activity.

Figure 5 The estimated respiratory activity (top) calculated by fastICA (bottom) calculated by RTpca.

Table 2 The detection rate of the periods without breathing in Experiment II as a percentage of the total number of events.

True positive	True negative	False negative	False positve
95.8%	94,8%	4.2%	5.2%

length of the estimated eigenvectors have been further used to detect the periods of the held breath in Experiment II. To do so, each major change in the length triggered a MATLAB script to detect the changes in breathing. By comparing the power spectral density of the lower frequencies, right before and right after the change of the EV length, the periods of holding the breath in Experiment II could be detected. Table 2 gives the results.

As was already indicated, the SCICA approach has also been tested as a new method to extract a respirational feature. The results are provided by Figures 5 and 6, allowing a direct comparison with the performance of the RTpca algorithm.

Discussion

The presented results are very promising with respect to the different applications. The conclusion drawn from
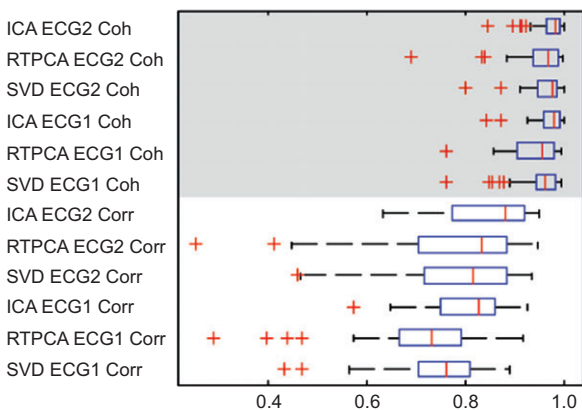

Figure 6 The RTpca, SVD, and SCICA performance in the respiratory component extraction from the different ECG leads. The boxplot shows the correlation and coherence of the estimated respiratory signal and respiratory reference signal.

the correlation of the changes in the length of the EV and ACC activity as presented in the previous section is twofold. First, we could immediately stop the learning process whenever there is a minimum activity within the ACC signals. When using the RTpca algorithm, this could be done by increasing the value of the parameter T (see Equation 4). This would require a measurement system as presented in this work though. Second, we also come to the conclusion that, instead of using an ACC signal as the indicator for the environmental changes, it is possible to configure a separate RTpca neuronal network, solely for the task of detecting the changes in the eigenvectors, which can be done by fixing the learning rate to a small constant value, as was done in the previous example. The information generated by this NN can then be used to coordinate the learning rates of another NN, which is supposed to track the actual eigenvectors instead.

Analyzing the results of the conducted respiratory experimentes, we can claim to extract a surrogate respiratory signal information out of a single-channel ECG online. Referring to the different ECG leads, in our data sets ECG II provided slightly better results than ECG I. In general, however, the leads most suited for respiratory estimation are known to change from subject to subject [20]. Moreover, several ideas that utilize single-channel ECG data to detect the obtrusive sleep apnea have been presented in [4]. As the approaches of this paper have proven successful in the detection of stops in breathing, it is conceivable that the changes in the properties of the online-estimated eigenvectors can endorse the tools used in sleep studies to indicate the incidence of apnea.

It strikes out that the achieved outcome of the SCICA is significantly better than the RTpca approach. Moreover, the SCICA outperforms the results obtained by SVD. Plot (B) in Figure 5 shows the estimated independent component that contains the respirational signal.

Conclusion

In this work, we have evaluated several adaptive approaches to solve the PCA expansion of single-lead ECG signals. We have been able to identify the RTpca algorithm as a proper and well-performing choice to estimate the

first four principal components. It was verified that a surrogate respiratory signal can be found in one of the PCs. Therefore, it is even conceivable to completely abstain from additional hardware to obtain a respiratory signal.

Further, the great improvement of the adaptive approach implemented in this work is the ability of online extraction of the respiratory component. This is a valuable property, especially when immediate processing of the sampled signals is required. We mentioned the application in sleep medicine as an interesting example that can capitalize on our results in terms of less hardware and online detection of the changing breath patterns that might assist in real-time apnea detection.

Not only the extraction of the respirational features but also the gathering of the other vital parameters like morphologic variability, which can be derived from the eigenvalue distribution as discussed in [3], can profit from the presented online approach.

Typically, adaptive approaches that rely on data-dependent learning rates are difficult to handle, as their output significantly depends on the current configuration.

An innovative measurement system has been proposed that, next to the physiological biosignals, also acquires acceleration data. This information can be used to reconfigure the learning rates and stop adaption in the noisy segments, for example, which enhances the performance as the system reconverges much faster.

Compared with the traditional approach of SVD, the computational load is significantly reduced as the online algorithms can be implemented on the resource-saving NN structures, thereby, being attractive for implementations on the low-performance systems like the mobile sensor nodes.

In a final step, the single-channel ICA approach was applied to extract the respiratory signal. In the first tests, a batch implementation of the fastICA algorithm clearly outperformed the PCA expansion approach in terms of accuracy. As online approaches of the fastICA algorithm exist, it seems promising to resort to an adaptive approach of the fastICA problem as well.

References

[1] Afonso V, Tompkins W, Nguyen T, Luo S. ECG beat detection using filter banks. IEEE Trans Biomed Eng 1999; 46(2): 192–202.

[2] Bowers E, Murray A, Langley P. Respiratory rate derived from principal component analysis of single lead electrocardiogram. Comput Cardiol 2008; 35: 437–440.

[3] Castells F, Laguna P, Sörnmo L, Bollman A, Roig J. Principal component analysis in ECG signal processing. EURASIP J Adv Signal Process 2007; 1: 98–119.

[4] Chazal P, Heneghan C, Reilly R, Nolan P, O'Malley M. Automated processing of the single-lead electrocardiogram for the detection of obstructive sleep apnoea. IEEE Trans Biomed Eng 2003; 50(6): 686–696.

[5] Chen L, Chang S. An adaptive learning algorithm for principal component analysis. IEEE Trans. Neural Netw 1999; 6(5): 1255–1263.

[6] Clifford G, Azuaje F, McSharry P. Advanced methods and tools for ECG data analysis. Norwood, USA: Artech House Inc. 2006.

[7] Davies M, James C. Source separation using single channel ICA. Signal Process 2007; 87(8): 1819–1832.

[8] Golub G, Loan C. Matrix computations, 2nd edition. Baltimore: The Johns Hopkins University Press 1989.

[9] Han D, Rao N, Principe C, Gugel K. Real-time PCA (principal component analysis) implementation on DSP. Neural Netw 2004; 3: 2159–2162.

[10] Haxter M. Entwicklung der Hard- und Software eines mobilen drahtlosen Atemfrequenzsensors und Implementierung von Algorithmen zur Unterdrückung von Signalartefakten, Diploma Thesis, Chair of Electronics and Medical Signal Processing, TU Berlin: 2011.

[11] Hyvärinen A, Oja E. A fast fixed-point algorithm for independent component analysis. Neural Comput 1997; 9: 1483–1492.

[12] Hyvärinen A, Oja E. Fast and robust fixed-point algorithms for independent component analysis. IEEE Trans Neural Netw 1999; 3: 626–634,

[13] Hyvarinen, Karhunen J, Oja E. Independent component analysis. New York: Wiley 2001.

[14] Joliffe I. Principal component analysis. New York: Springer 2002.

[15] Kung S, Diamantaras K. A neural network learning algorithm for adaptive principal component extraction (APEX). Proc. Int Accoustics, Speech Signal Processing ICASSP-90: 861–864.

[16] Langley P, Bowers E, Murray A. Principal component analysis as a tool for analyzing beat-to-beat changes in ECG features: application to ECG-derived respiration. IEEE Trans Biomed Eng 2010; 57(4): 821–829.

[17] Oja E. Principal components, minor components, and linear neural networks. Neural Netw 1992; 5: 927–935.

[18] Pflugradt M, Mann S, Feller V, Orglmeister R. On-line learning algorithms for extracting respiratory activity from single lead ECGs based on principal component analysis. Bio Med Technol 2012; 57: 352–354.

[19] PhysioNet PhysioBank ATM, the research resource for complex physiologic signals, Available at: http://www.physionet.org/cgi-bin/atm/ATM. Accessed on 12 October, 2012.

[20] Pinciroli F, Rossi R, Vergani L, Carnevali P, Mantero S, Parigi O. Remarks and experiments on the construction of respiratory waveforms from electrocardiographic tracings. Comput Biomed Res 1986; 19: 391–409.

[21] Queisser S. Aufbau eines mehrkanaligen EKG-Sensormoduls zur Integration in ein Body Sensor Network und Entwicklung eines Funkprotokolls angelehnt an den Standard IEEE 802.15.4, Master's Thesis, Chair of Electronics and Medical Signal Processing, TU Berlin: 2011.

[22] Rao Y, Principe J. A fast on-line algorithm for PCA and its convergence characteristics. Proc. NNSP X 2000; 1: 299–307.

[23] Sanger T. Optimal unsupervised learning in a single-layered linear feedforward network. Neural Netw 1989; 2: 459–473.

[24] Texas Instruments. MSP430F161x Mixed Signal Microcontroller. Datasheet SLAS368G, Available at: http://www.ti.com/lit/ds/symlink/msp430f1611.pdf March 2011. Accessed on 12 October, 2012.

[25] Yang B. Projection approximation subspace tracking. IEEE Trans Sig Proc J SP 1995; 43: 95–107.